Ultrafast time-resolved imaging of femtosecond laser-induced periodic surface structures on GaAs

Xin Jia (贾 鑫)[1,2], Yanhong Yuan (袁艳红)[1], Dangqiang Yang (杨党强)[1], Tianqing Jia (贾天卿)[2], and Zhenrong Sun (孙真荣)[2]

[1]*Department of Mathematics and Physics, Shanghai Dianji University, Shanghai 201306, China*

[2]*State Key Laboratory of Precision Spectroscopy, East China Normal University, Shanghai 200062, China*

Corresponding author: jiaxin@sdju.edu.cn

Received June 22, 2014; accepted August 8, 2014; posted online October 28, 2014

We report the formation dynamics of periodic ripples on GaAs induced by femtosecond laser pulses (800 nm, 50 fs) via a collinear time-resolved imaging technique with a temporal resolution of 1 ps and a spatial resolution of 440 nm. The onset of periodic ripples emerges in the initial tens of picoseconds in the timescale of material ejection. The periodic ripples appear after irradiation of at least two pump pulses at surface defects produced by the first pulse and the ripple positions kept stable until the formation processes complete. The formation mechanisms of laser-induced periodic ripples are also discussed.

OCIS codes: 320.7130, 100.0118, 160.6000.
doi: 10.3788/COL201412.113203.

Recently, laser-induced periodic surface structures (LIPSSs) by femtosecond (fs) pulses have become a good technology for producing a large variety of structured materials. Generally, two kinds of surface structures were induced by fs pulses at appropriate laser fluences and pulse numbers: low spatial frequency LIPSS (LSFL) with spatial periods of 0.5–0.95 λ and high spatial frequency LIPSS (HSFL) of 0.1–0.5 λ. HSFL were studied intensely for the short spatial periods and the puzzling formation mechanisms[1–5]. Surface morphology with LSFL have also received much research attention owing to the abilities to produce novel materials with improved optical properties[6–13], such as black silicon embedded with microspikes[6,7], colored metals due to the formation of submicron ripples[8], and absorption-enhanced semiconductors by the micro-holes array[9,10].

The formation of ripple structures induced by continuous wave or nanosecond laser was explained by the interference of incident laser beam with the surface scattered light wave[14]. However, many different phenomena of fs laser-induced LSFL cannot be well explained by the classical scattering model. For example, the ripple periods changed in the range of 0.5–0.95 λ for normal incident laser and decreased with increasing the irradiated pulses[14]. The formation mechanism of fs laser-induced LSFL is still an open problem and many experimental and theoretical studies have been devoted to the formation of LSFL[15–17]. In addition, several models, such as second harmonics in the surface[17], standing wave in the material subsurface layer[18], and splitting of LSFL[19,20], have also been proposed that the formation of HSFL involved the emergence of LSFL. Therefore, the studies on the formation of LSFL benefit the understanding of fs laser-induced surface structures and contribute to the control of laser structured surface morphology.

Pump–probe technique is a useful method to study the ultrafast dynamics of melting and ablation irradiated by fs laser pulses[21–26] fs time-resolved pump–probe diffraction was performed to study the temporal evolution of LSFL formation in silica glass induced by 800 nm fs laser[24]. Using a non-collinear pump–probe imaging technique, Murphy *et al.* observed LSFL formation on Si surface on the same timescale as material removal[25].

Using a collinear pump–probe imaging technique, we have studied the evolution processes of LSFL formation on Si surface[26]. In this letter, we report the temporal evolution of LSFL formation on GaAs by using the same collinear pump–probe imaging technique, in which a 100× microscope (numerical aperture (NA) = 0.9) was used to promote the spatial resolution to 440 nm. We observed the timescale of LSFL formation and revealed the influence of pre-existing surface structures on the subsequent ripples formation. The results confirmed the similar evolution processes of fs laser-induced surface periodic ripples on different materials and devoted to the physical mechanisms of ripple formation.

A commercial Ti:sapphire regenerative amplifier laser system (Legend Elite, Coherent) generated 800 nm, 50 fs, 10 Hz laser pulses with a maximum pulse energy of 3.5 mJ. The laser beam was split into two beams by a beam splitter. One laser beam was employed as the "pump" beam to induce surface structures on GaAs and the other was focused into a 10 mm thick water cell to stimulate a white-light beam, which was referred to as "probe" beam and served as the illumination source. Then, the pump and probe beams were collinearly input into a microscope (Nikon, 80*i*) and the reflected surface images were observed by a charge-coupled device (CCD) camera. An objective lens (100×, NA = 0.9) was used to focus the pump and

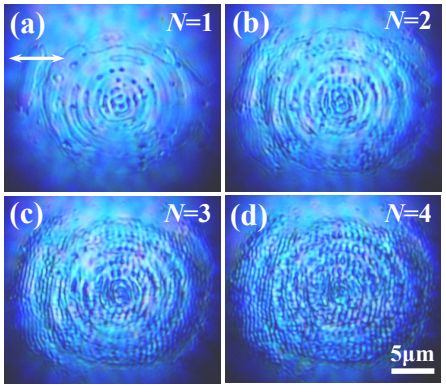

Fig. 1. Optical micrographs of solidified surface structures by 1–4 shots of pump pulse at a laser fluence of 0.45 J/cm^2. The horizontal arrow in (a) indicates the laser polarization direction.

probe beams at normal incidence on GaAs surface in air so that the spatial resolution was promoted to 440 nm. The white light beam was temporally dispersive in the water cell and objective lens, and the probe pulse was estimated to be ~1 ps, which determined the temporal resolution. The experimental details can be found in Ref. [26].

A commercial available undoped GaAs (110; MTI-group, China) with a thickness of 0.45 mm was used in the experiment. Single surface was optically polished with a roughness less than 10 nm. The sample was mounted on an XYZ translation stage.

Figure 1 shows the optical micrographs of ablated spot after irradiation by 1–4 pump pulses. The blue images are due to a short wave pass filter with a cutoff at 600 nm in front of the CCD camera. After single shot, the annular structures are ablated due to the diffraction of the lens (Fig. 1(a)). Few LSFLs begin to emerge in the direction perpendicular to the laser polarization by two shots. With the pulse number increasing to 3, clear and regular LSFLs are observed with a spatial period of 520 nm. As $N = 4$, abundant longer LSFLs appear.

Figure 1 shows that LSFLs are induced by at least two shots of pump pulse. Therefore, we observe the time-resolved micrographs of surface structures after irradiation of the second pump pulse at different delay times, as shown in Fig. 2. Each image is obtained in a different irradiated area of the sample. Before arrival of the second pump pulse, Fig. 2(a) shows that only surface defects produced by the first pump pulse are observed. The surface morphology does not change obviously before 20 ps (Figs. 2(b) and (c)). At 30 ps, the ring regions become a little dark, which originate from the intense absorption of both charged particles and neutral atoms ejecting from the molten surface[21–23,25,26]. The onset of LSFL is found in the ring regions by 70 ps (see red ellipses in Fig. 2(e)). With the time passing, LSFLs grow more legibly on the darker surface as more materials eject (Fig. 2(f)). The surface becomes darkest at about 600–2000 ps, while the surface morphologies are blocked by the ejected material, as shown in Figs. 2(g) and (h).

We compare the optical micrographs of before, 70 ps, and after irradiation of the second pump pulse to obtain the spatial information during the LSFL formation, as shown in Fig. 3. Figures 3(a) and (b) indicate that LSFL begin to emerge on the surface defects produced by the first pump pulse. Figure 3(d) shows the intensity curves of CCD pixels along the respective red arrows in Figs. 3(a)–(c). The relatively smooth "before" curve in Fig. 3(d) indicates almost no ripple before the arrival of the second pump pulse. The periodic fluctuation of "70 ps" curve demonstrates the emergence of ripples with a period of about 520 nm, and the accordance of "70 ps" and "after" curves provides evidences of stable ripple positions during formation process.

Clear and regular LSFLs are observed by three shots (Fig. 1(c)), so the temporal evolution of LSFL irradiated by the third pump pulse is also measured, as shown in Fig. 4. The evolution process is similar to that of the

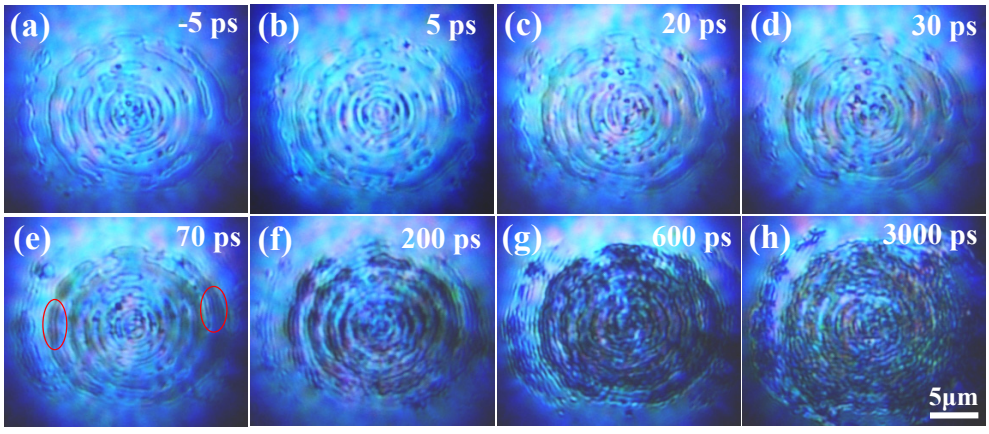

Fig. 2. Optical micrographs of sample surface after irradiation of the second pump pulse with a laser fluence of 0.45 J/cm^2 at different delay times.

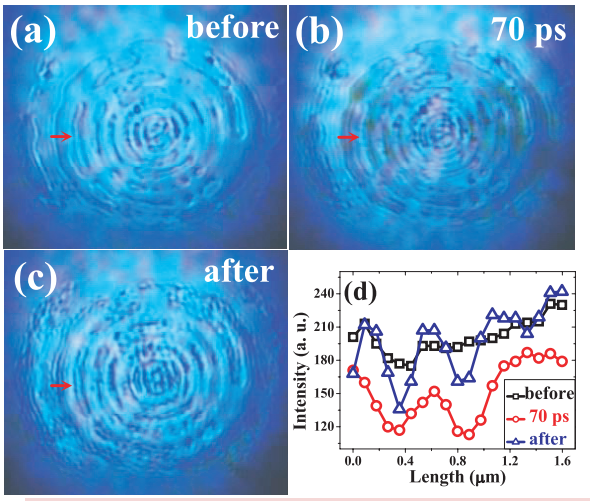

Fig. 3. Optical images at (a) before, (b) 70 ps, and (c) after irradiation of the second pump pulse, respectively. The respective red arrows in (a)–(c) mark the same positions. (d) Intensity curves of CCD pixels along the arrows.

second pump pulse. The micrograph shown in Fig. 4(a) indicates that the surface micrographs remain almost unchanged before 20 ps and the dark regions due to material ejection appear at 30 ps (Fig. 4(b)). From then on, the destroyed regions become much darker, and the onset of LSFL is found at ~ 90 ps. More longer ripples form on the darker surface at 200 ps. The surface morphologies are shielded by the ejected material since 600 ps, as shown in Figs. 4(e) and (f).

Figures 5(a)–(c) show the optical micrographs of before, 90 ps, and after irradiation of the third pump

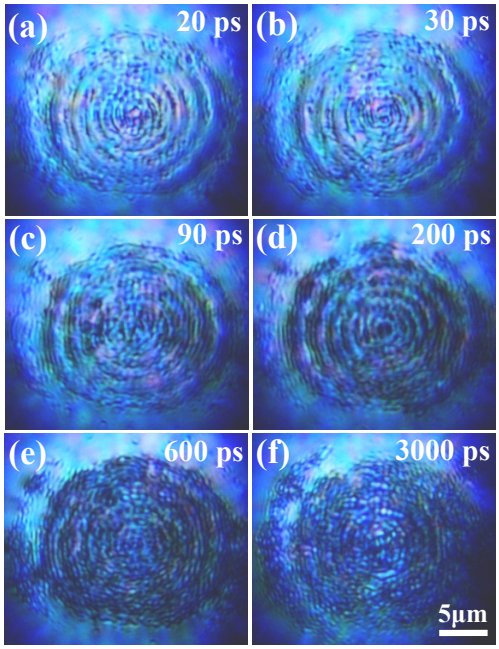

Fig. 4. Optical micrographs of sample surface after irradiation of the third pump pulse with a laser fluence of 0.45 J/cm² at different delay times.

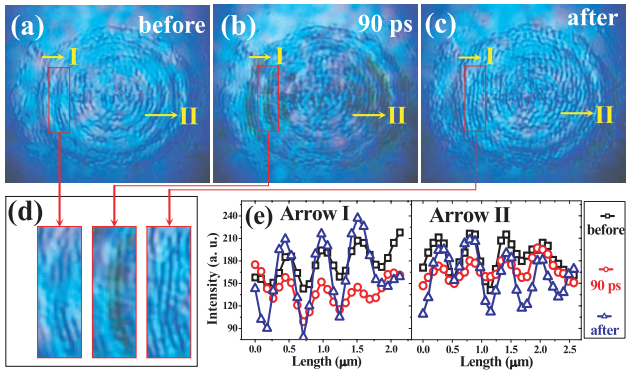

Fig. 5. Optical images at (a) before, (b) 90 ps, and (c) after irradiation obtained a few seconds before the arrival and a few seconds after irradiation of the third pump pulse, respectively. The laser fluence is 0.45 J/cm². The respective boxes and arrows in (a)–(c) mark the same positions. (d) Magnified images of the red boxes in (a)–(c). (e) Intensity curve of CCD pixels along the respective arrows "I" and "II" in (a)–(c).

pulse for the purpose of understanding the influence of the pre-existing ripples on the formation of subsequent LSFL. The magnified images for the same part of ablation spot in Figs. 5(a)–(c) are shown in Fig. 5(d), from which it can be found that LSFLs grow longitudinally and the adjacent ripples link to each other during evolution processes. Figure 5(e) shows the intensity curves of CCD pixels along the respective arrows "I" and "II" in Figs. 5(a)–(c), where the pre-existing ripples have been induced by the first two pump pulses. The larger amplitude of "after" curve than that of "before" qualitatively indicates the increasing depth of the LSFL, while the amplitude of "90 ps" curve is obviously small due to the shaded LSFL by material ejection. The consistent positions of the crests and grooves of respective curves in Fig. 5(e) along the respective arrows "I" and "II" demonstrate that the ripple positions remain stable during the formation processes. The temporal evolution of the LSFL formation by the fourth shot is nothing different from that of the third one, except for the existence of more abundant ripples.

From the experimental results of the pump–probe imaging, it is inferred that thermodynamics and hydrodynamics effects act rarely on the ripple formation because of scarce movement of ripples[26]. Additionally, the experimental results show that LSFLs appear after irradiation of the second pump pulse, and the onset of LSFL emerges at several tens of picoseconds. These phenomena indicate that the ripples are mainly determined by the initial process of a non-uniform energy deposition of the pump pulse, and the modulation of energy deposition may be introduced by the surface defects during the interaction between laser pulse and material. At present, several models, such as interference between laser-induced surface plasmon and incident laser[15], capillary instability in the surface molten layer[16], and scattering of

rough surface[17], have been proposed to explain the modulation of laser energy deposition, which needs further experimental and theoretical works.

In conclusion, we study the formation dynamics of fs laser-induced LSFL on GaAs surface using a collinear time-resolved imaging technique. The onset of periodic ripples emerges in the initial tens of picoseconds after irradiation in the timescale of material ejection. Additionally, LSFLs appear by irradiation of at least two pump pulses and the ripple positions remain stable during the evolution processes. These results indicate that the periodic energy deposition in GaAs surface introduced by the structured surface plays a dominant role in the formation of LSFL.

This work was supported by the National Natural Science Foundation of China (Nos. 11104178, 11274116, and 51132004), the National Special Science Research Program of China (Nos. 2010CB923203 and 2011CB808105), the Innovation Program of Shanghai Municipal Education Commission (Nos. 14YZ156, 11JC1403500, and 10XD1401800), the Young Teacher Program of Shanghai University (No. shdj006), and the Discipline Foundation Project of Shanghai Dianji University (No. 12XKJC01).

References

1. A. Borowiec and H. K. Haugen, Appl. Phys. Lett. **82,** 4462 (2003).
2. Q. Z. Zhao, S. Malzer, and L. J. Wang, Opt. Lett. **32,** 1932 (2007).
3. Y. Yang, J. Yang, L. Xue, and Y. Guo, Appl. Phys. Lett. **97,** 141101 (2010).
4. K. Miyazaki and G. Miyaji, J. Appl. Phys. **114,** 153108 (2013).
5. J. Z. P. Skolski, G. R. B. E. Romer, J. V. Obona, and A. J. Huis in't Veld, J. Appl. Phys. **115,** 103102 (2014).
6. R. Younkin, J. E. Carey, E. Mazur, J. A. Levinson, and C. M. Friend, J. Appl. Phys. **93,** 2626 (2003).
7. C. Wu, C. H. Crouch, L. Zhao, J. E. Carey, R. Younkin, J. A. Levinson, E. Mazur, R. M. Farrell, P. Gothoskar, and A. Karger, Appl. Phys. Lett. **78,** 1850 (2001).
8. A. Y. Vorobyev and C. Guo, Laser Photon. Rev. **7,** 385 (2013).
9. X. Jia, T. Q. Jia, Y. Zhang, P. X. Xiong, D. H. Feng, Z. R. Sun, and Z. Z. Xu, Opt. Express **18,** 14401 (2010).
10. Y. Zhang, X. Jia, P. X. Xiong, and T. Q. Jia, Chin. Opt. Lett. **8,** 1203 (2010).
11. K. Lou, S. Qian, X. Wang, Y. Li, B. Gu, C. Tu, and H. Wang, Opt. Express **20,** 120 (2012).
12. L. Yang, Y. Wang, and L. Zhao, Chin. Opt. Lett. **10,** 063102 (2012).
13. S. Zhang, X. Hu, Y. Liao, F. He, C. Liu, and Y. Cheng, Chin. Opt. Lett. **11,** 033101 (2013).
14. D. Emmony, R. Howson, and L. Willis, Appl. Phys. Lett. **23,** 598 (1973).
15. M. Huang, F. L. Zhao, Y. Cheng, N. S. Xu, and Z. Z. Xu, ACS Nano **3,** 4062 (2009).
16. M. Y. Shen, C. H. Crouch, J. E. Carey, and E. Mazur, Appl. Phys. Lett. **85,** 5694 (2004).
17. D. Dufft, A. Rosenfeld, S. K. Das, R. Grunwald, and J. Bonse, J. Appl. Phys. **105,** 034908 (2009).
18. X. Jia, T. Q. Jia, Y. Zhang, P. X. Xiong, D. H. Feng, Z. R. Sun, J. R. Qiu, and Z. Z. Xu, Opt. Lett. **35,** 1248 (2010).
19. Y. Y. Huo, T. Q. Jia, D. H. Feng, S. A. Zhang, J. K. Liu, J. Pan, K. Zhou, and Z. R. Sun, Laser Phys. **23,** 056101 (2013).
20. M. Huang, Y. Cheng, F. L. Zhao, and Z. Z. Xu, Ann. Phys. **525,** 74 (2013).
21. M. C. Downer, R. L. Fork, and C. V. Shank, J. Opt. Soc. Am. B **2,** 595 (1985).
22. K. Sokolowski-Tinten, J. Bialkowski, A. Cavalleri, D. von der Linde, A. Oparin, J. Meyer-ter-Vehn, and S. I. Anisimov, Phys. Rev. Lett. **81,** 224 (1998).
23. V. V. Temnov, K. Sokolowski-Tinten, P. Zhou, and D. von der Linde, J. Opt. Soc. Am. B **23,** 1954 (2006).
24. S. Höhm, A. Rosenfeld, J. Kruger, and J. Bonse, Appl. Phys. Lett. **102,** 054102 (2013).
25. R. D. Murphy, B. Torralva, D. P. Adams, and S. M. Yalisove, Appl. Phys. Lett. **103,** 141104 (2013).
26. X. Jia, T. Q. Jia, N. N. Peng, D. H. Feng, S. A. Zhang, and Z. R. Sun, J. Appl. Phys. **115,** 143102 (2014).